



THE UNIVERSITY *of* EDINBURGH

Edinburgh Research Explorer

Materials for near-IR light modulation

Citation for published version:

Zamboni, R (ed.), Kajzar, F (ed.), Szep, AA (ed.), Matczyszyn, K (ed.), Whyte, AM & Robertson, N 2016, 'Materials for near-IR light modulation', pp. 999404. <https://doi.org/10.1117/12.2241738>

Digital Object Identifier (DOI):

[10.1117/12.2241738](https://doi.org/10.1117/12.2241738)

Link:

[Link to publication record in Edinburgh Research Explorer](#)

Document Version:

Peer reviewed version

General rights

Copyright for the publications made accessible via the Edinburgh Research Explorer is retained by the author(s) and / or other copyright owners and it is a condition of accessing these publications that users recognise and abide by the legal requirements associated with these rights.

Take down policy

The University of Edinburgh has made every reasonable effort to ensure that Edinburgh Research Explorer content complies with UK legislation. If you believe that the public display of this file breaches copyright please contact openaccess@ed.ac.uk providing details, and we will remove access to the work immediately and investigate your claim.



Materials for near-IR light modulation

Alexander M. Whyte^a, Neil Robertson^{*a}

^aEaStCHEM School of Chemistry, University of Edinburgh, King's Buildings, Edinburgh EH9 3FJ

ABSTRACT

The work reported outlines the synthesis, film formation and application of NIR-absorbing metal dithiolene and metal diimine molecules suitable for film formation with varying ligands and central metals. Formation of an electroactive film on conducting glass or mesoporous TiO₂ support can be achieved through electropolymerisation, electrodeposition, spin/drop coating or chemical attachment. In this context, we will outline the synthesis, characterisation and properties of a new family of NIR-absorbing aromatic metal diimine complexes. These complexes are shown to give rise to planar, delocalised structures with small HOMO-LUMO gaps, through the use of extended non-innocent ligands *o*-semibenzoquinonediimines. Herein we report the synthesis of a series of metal diimine complexes, modified to extend the electronic conjugation and shift the intense low-energy absorption from the visible to the NIR region. This study extends the range of available NIR absorbing metal-complex chromophores and opens up new possibilities for wavelength tuning and application.

Keywords: Near-IR, electrochromism, diimine complex, dithiolene complex

1. INTRODUCTION

There are a number of important applications of near-IR chromophores in civilian and in military applications. These include as Q-switch laser dyes;¹ protection of sensors and the eyes of personnel to intense laser pulses over a broad wavelength;² as filters to improve the contrast in night-vision imaging systems to avoid interference from stray near-IR radiation from displays;² electrochromic near-IR films for thermal control of buildings by modulating the near-IR radiation transmitted;³ optoelectronic memory and information storage achieved using films that possess different stable redox states with different near-IR absorption;⁴ light absorption at telecommunication wavelengths;¹ and non-linear optics along with electrochromic switching.⁵

Metal dithiolene complexes have been extensively studied as near-IR dyes,⁷ principally as Q-switch dyes for lasers⁸ due to their strong NIR absorption and their stability to intense laser light. It has been shown that the low energy absorption can be tuned through modification of peripheral groups on the ligand or by changing the central metal. Also, with appropriate design, visible-transparent dyes can be prepared with intense near-IR absorption. We are only aware however of one example of the electrochromic switching of the near-IR absorption of dithiolene complexes in thin-film form, previously reported by our group.⁹ This was achieved through electropolymerisation of indole units, leading to robust organic films on the working electrode (Figure 1a). In addition, we have also used an electrodeposition method to form robust thin films of dithiolene complexes, achieved by oxidising a soluble monoanionic complex at an electrode to form the insoluble neutral species.⁶ Remarkable near-IR absorption out to around 2000 nm was observed in the resulting thin films of Ni and Cu-complexes (Figure 1b). This demonstrates the extended absorption that can occur due to intermolecular interactions between the planar molecules. In both of these examples, the films remained sufficiently conducting to enable film growth and also in the former case to allow rapid electrochromic switching. To date however, there have been limited families of near-IR absorbing metal complex dyes and hence limited opportunity to tune and optimise properties. In the case of the closely-related metal-*bis*-1,2-diimine complexes, although they have been studied as visible-absorbing chromophores for NLO, they do not typically show NIR absorption. In this work, we describe the synthesis and characterisation of new examples of metal-diimine complex dyes, leading to novel near-IR absorption, opening up a new family of molecules suitable for further study and variation.

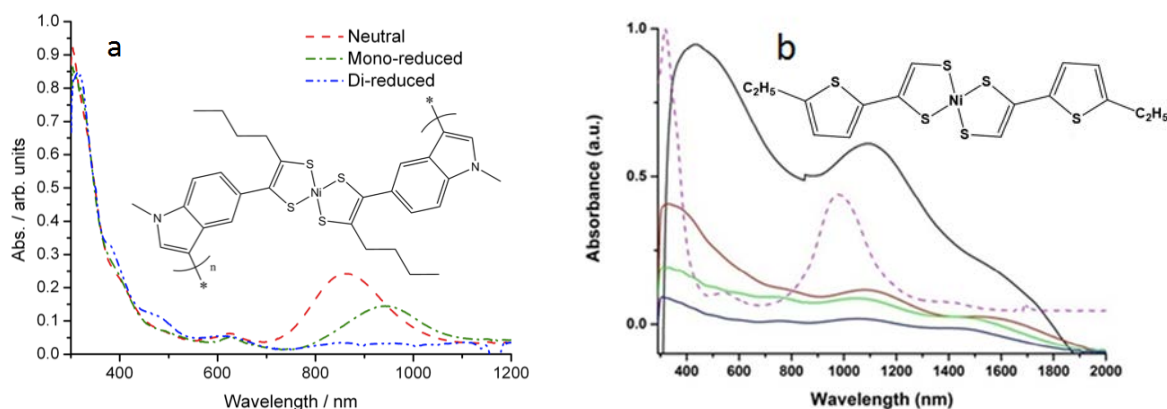


Figure 1 (a) Molecular structure and electrochromic switching of neutral and reduced metal-*bis*-1,2-dithiolene complex;⁹ and (b) molecular structure and various film thicknesses (solid lines) of an electrodeposited metal-*bis*-1,2-dithiolene complex compared with the monoanionic complex in solution (dashed line).⁶

2. RESULTS AND DISCUSSION

Aromatic diimine complexes have been shown to give rise to planar, delocalised structures with small HOMO-LUMO gaps, through the use of non-innocent ligands such as *o*-semibenzoquinonediimine (shown in Figure 2 as L^1).^{10,11,12} Work by Noro *et al.*^{13,14} illustrated the potential application for use of bis(*o*-diiminobenzosemiquinonate) nickel(II) in thin film transistors. This complex possessed a small HOMO-LUMO gap of *ca.* 0.8 V, giving rise to ambipolar charge transport with respectable hole and electron mobilities in the range of 10^{-3} to 10^{-2} $\text{cm}^2 \text{V}^{-1} \text{s}^{-1}$.

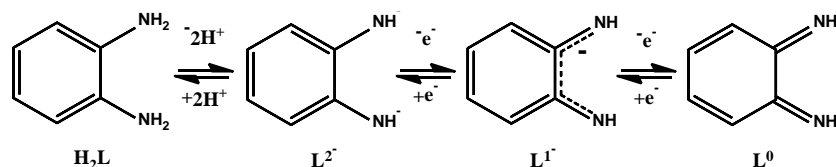


Figure 2 The various resonance forms of *o*-phenylene diamine upon protonation and subsequent oxidation.

Variations to this parent compound to tune the electronic properties could be achieved by exchanging the central metal ion, varying the substituents on the semibenzoquinonediimine ligand or expanding the π -conjugation of the system by using a diamino naphthalene or phenanthrene ligand. A series of bis-ligand diimine Ni(II) complexes was reported in 1989 by Lelj *et al.* using 2,3-diiminonaphthalene (*din*) and 9,10-diiminophenanthrene (*dip*) as ligands. This study focused on the conductivity of the three complexes in iodinated pressed pellets, with the authors reporting that the conductivity of $\text{Ni}(\text{dip})_2\text{I}_x$ was 10^3 - 10^4 times greater than that of the analogous iodinated phenylenediimine Ni(II) compound.¹⁵ However, to the best of our knowledge there exists no studies exploring this type of complex as potential near-IR dyes, which we expect may be achieved by extending the conjugation of the core delocalised unit. Accordingly we report herein the synthesis of modified *o*-phenylenediimine metal complexes using the ligand 4,5-bis(dodecyloxy)benzene-1,2-diamine, possessing additional alkoxy groups to extend the electronically delocalised motif with additional electron donor units. In addition, the inclusion of alkyl chains in these species may facilitate film formation through spin or drop coating.

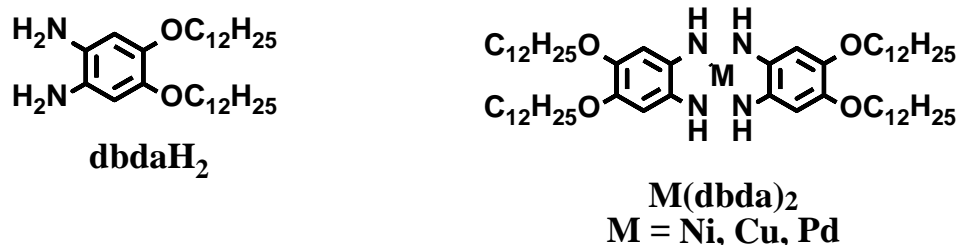


Figure 3 Structures of the molecules reported in this work.

Bis-ligand Ni, Cu and Pd complexes, M(dbda)₂, were prepared and were found to exhibit NIR absorptions, attributed to the small energy gap between their HOMO and LUMO (*vide infra*). The formation of the desired species was confirmed by mass spectrometry, with the expected molecular ion peak, and associated isotopic splitting pattern observed for each complex. The proton NMR signals from the Ni(II) and Pd(II) complexes appear broad, with no resolution of peak multiplicity, quite unlike the NMR spectrum obtained for the free ligand, H₂dbda. This may be due to aggregation effects of the planar complexes in solution. The complexes were purified by size exclusion chromatography using a long column (~ 1 m) and in the case of all three M(dbda)₂ complexes two fractions were observed. The first fraction, brown in colour, was discarded whereas the second fraction was found to contain the desired compound and had a characteristic colour pertaining to that particular molecule. In all cases the fraction containing the desired complex was then rechromatographed. Each of the diimine complexes, as well as the free ligand used in the synthesis of these molecules, has a tendency to gradually decompose in the presence of air and light, even when stored under N₂. Some difficulty was encountered in obtaining satisfactory microanalysis for the complexes Cu(dbda)₂ and Pd(dbda)₂, presumably due to the sensitivity in air. Prior to carrying out any studies the materials were first columned as a precautionary measure to ensure that there was no decomposed material present prior to commencing any measurements. As a consequence of the uncertainty surrounding the stability and purity of the majority of the Cu and Pd complexes, this initial study is focused primarily on Ni(dbda)₂.

The complex Ni(dbda)₂ was characterised using cyclic voltammetry (CV) and differential pulse voltammetry (DPV) as shown in Figure 4. The compound exhibits several facile redox processes occurring within the solvent window. Starting with the cyclic voltammetry measurements, on scanning to 0.5 V (vs. Ag/AgCl) an oxidative process was witnessed at 0.28 V with the associated return wave at 0.17 V. The process appears to be chemically reversible but the peak to peak separation of 110 mV is too large for the process to be considered electrochemically reversible. On increasing the scan rate the peak current of the forward and reverse processes grow with a slight shift in the peak position; on the forward scan at 0.1 V/s the peak position is at 0.28 V but applying a scan rate of 1 V/s causes the peak maximum to shift to 0.32 V. Likewise with the return wave, at 0.1 V/s the peak maximum is at 0.17 V but at 1 V/s the peak maximum is measured at 0.14 V. On applying negative potentials a reductive process is witnessed at -0.73 V with no return wave associated with this process. On inspection of the working electrode after scanning to -1 V an off-white, sticky film had been deposited onto the electrode indicating sample decomposition had occurred.

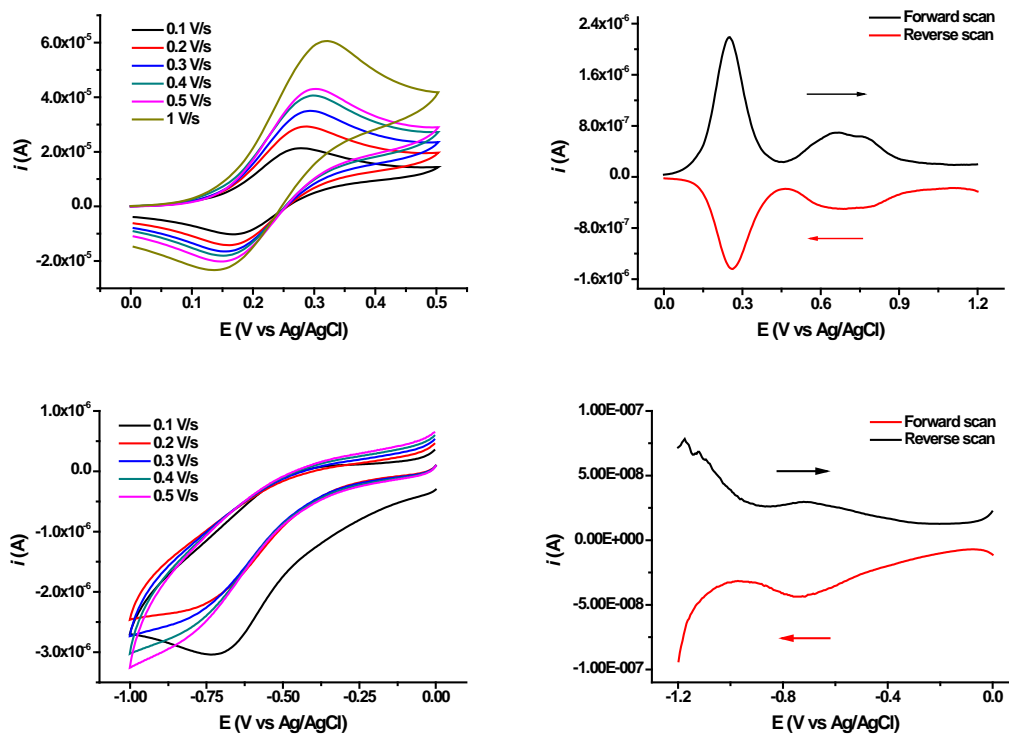


Figure 4 Cyclic voltammetry between 0 and 0.5 V (top left), and 0 and -1 V (bottom left) and differential pulse voltammogram of Ni(dbda)₂ between 0 and 1.2 V (top right), and between 0 and -1.2 V (bottom right). Measurements carried out in 0.3 M DCM with TBABF₄ supporting electrolyte.

Similar to the cyclic voltammetry analysis, differential pulse voltammetry from 0 to 1.2 V also highlights the occurrence of a facile oxidative process at 0.25 V. On further scanning to positive potentials, a second oxidation is witnessed. This appears as a broad, poorly defined peak with a mid-point at approximately 0.7 V (shown in Figure 4, top right). On reversing the direction of the scan and sweeping from 1.2 to 0 V the associated return waves from the oxidative processes are witnessed, indicating there is a degree of chemical reversibility attributed to both oxidative processes. Scanning from 0 to -1.2 V highlights the reductive process at -0.73 V, which reappears on the reverse scan from -1.2 to 0 V (Figure 4, bottom right). The electrochemical gap, between the first oxidation and first reduction, of around 1.0 V is indicative of a narrow HOMO-LUMO gap consistent with the possibility of near-IR absorption.

In keeping with the above, Ni(dbda)₂ displays a strong transition in the NIR region with lambda max at 1024 nm in DCM (Figure 5, left). Also, shown in the same Figure is the spectrum produced from the free ligand, dbdaH₂, in DCM, which shows no absorptions in the visible or NIR region. From the Beer-Lambert plot of Ni(dbda)₂ (Figure 5, right), the molar extinction coefficient has been calculated to be approximately 8500 L mol⁻¹ cm⁻¹. The straight line fit of absorbance vs. concentration also indicates that this transition at 1024 nm is not the result of aggregation of molecules in solution, and is therefore not an intermolecular transition. Additional transitions were witnessed at 299 and 535 nm. The effect of solvent on the observed absorption spectra is shown in Figure 6, however, only slight differences were observed in the peak position of the low-energy transition. The peak position changed from 1024 nm in DCM, 1,2-dichloroethane and 1,2-dichlorobenzene to 971 nm in hexane and diethyl ether. In toluene this transition appeared at 1011 nm. The trend appears to indicate positive solvatochromism, where the peak position displays a bathochromic shift with increasing solvent polarity. The transitions within the UV and visible region appear largely unaffected by the solvents used and no change in the complex's appearance was noted by optical inspection. The compound has limited solubility in polar solvents such as DMF and alcohols but is more readily solubilised in chlorinated solvents compared to non-polar solvents such as hexane, diethyl ether and toluene.

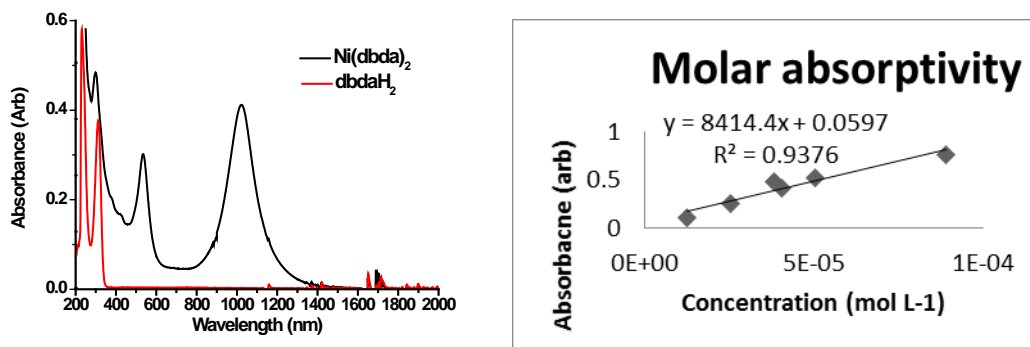


Figure 5 $\text{Ni}(\text{dbda})_2$ and dbdaH_2 absorption spectra in DCM between 200 and 2000 nm (left) and Beer-Lambert law plot of Absorbance vs. Concentration for the charge transfer process observed at λ_{max} of 1024 nm in the spectra of $\text{Ni}(\text{dbda})_2$ (right).

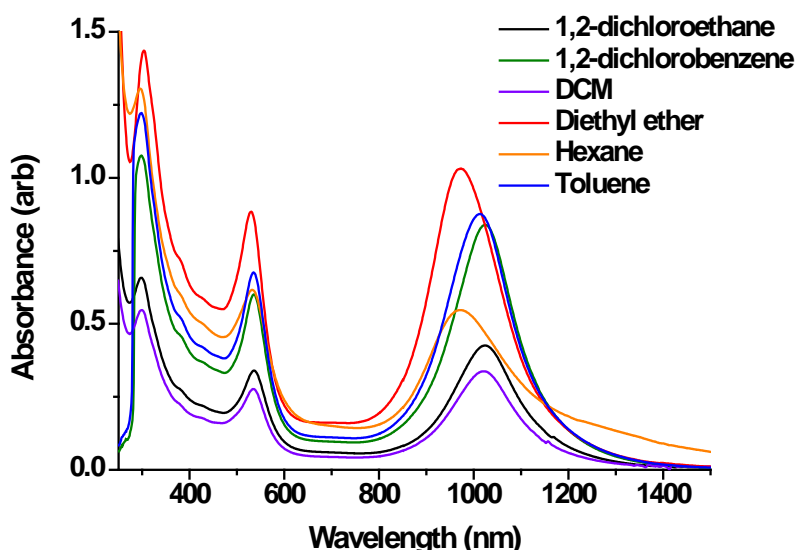


Figure 6 Absorption spectroscopy of $\text{Ni}(\text{dbda})_2$ in various non-polar or low-polarity solvents.

Thin-film absorption spectra of $\text{Ni}(\text{dbda})_2$ films deposited onto glass slides are shown in Figure 7. Solutions of 12 mg/L of $\text{Ni}(\text{dbda})_2$ in 1,2-dichlorobenzene were deposited onto both untreated and OTS treated glass substrates using drop casting and spin coating methods. The effect of surface treatment on the absorption spectra was compared when drop casting material onto a glass substrate (Figure 7, top left); the compound was deposited onto both a clean glass slide and another glass slide that had been subjected to OTS treatment. The resulting spectra appear identical regardless of whether or not surface treatment was employed, although the peak intensity was increased in the OTS coated film, likely due to a difference in film thickness associated with the limitations of the drop casting method for thin film preparation. Films were also prepared by spin coating from the same solution and the effect of annealing on the resulting absorption spectra was studied (Figure 7, top right). Two films were prepared on cleaned glass, as described earlier, with one glass film annealed at 150 °C for 3 minutes under a blanket of N_2 following sample deposition. However, both spectra appear identical with transitions occurring at 533 and 983 nm regardless of annealing, indicating that thermal treatment at that temperature has no effect on the structural order of the thin film. Films were also prepared by spin coating onto OTS treated glass slides (Figure 7, bottom) and the effect of thermal annealing compared. The red line shows the absorption

spectra of the as prepared thin film; it appears broad and featureless but after annealing at 150 °C for 3 minutes under a blanket of N₂, transitions at 533 and 983 nm can be resolved (Figure 7, bottom). This may be the result of a restructuring of the film associated with the interaction between the OTS SAM and the compound of study. The solution studies indicate that the NIR transition undergoes a bathochromic shift in chlorinated solvents compared with the thin film spectra, with the thin film spectra more closely resembling measurements carried out in solvents such as hexane and diethyl ether. In contrast to related metal-*bis*-1,2-dithiolene films however (Figure 1b), little intermolecular interaction appeared to occur with the film spectra broadly similar to those in solution.

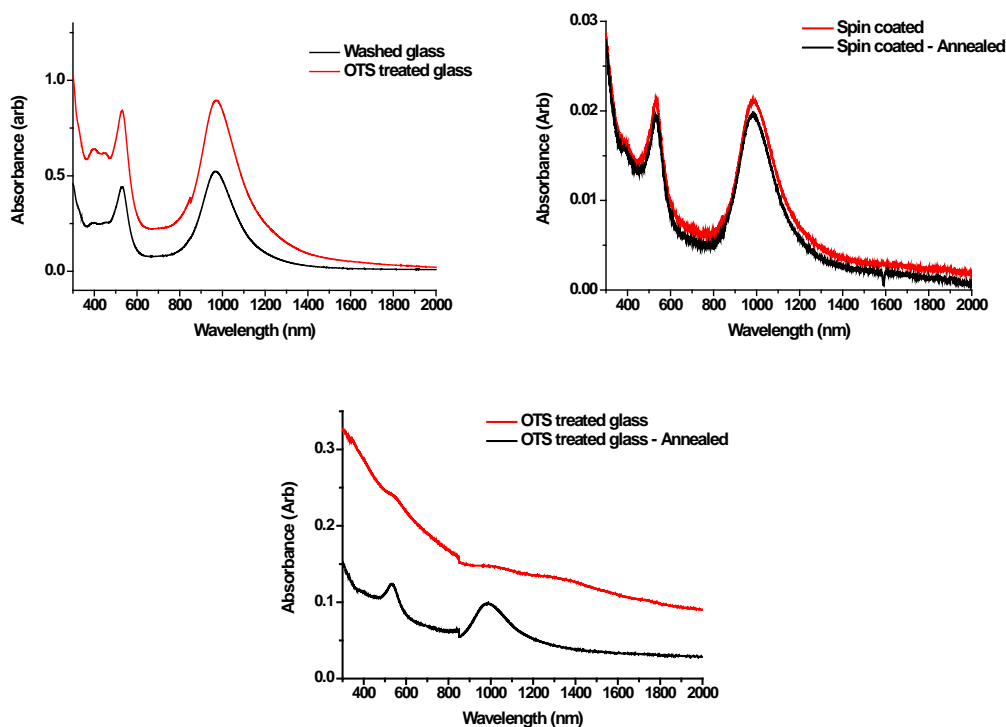


Figure 7 Thin film absorption spectra of Ni(dbda)₂ dropcast onto washed glass and OTS treated glass substrates (top, left), spin coated onto washed glass substrates (top, right) and spin coated onto OTS treated glass (bottom, centre). All measurements carried out between 2000 and 300 nm.

Differential scanning calorimetry (DSC, Figure 8) was carried out on Ni(dbda)₂ to investigate whether the complex exhibited any phase transitions between 25-350 °C. At 175 °C the onset of a small peak, corresponding to an exothermic process, was observed with a peak minimum at 182 °C. This process is likely due to the sample melting. Following this a large endothermic transition was observed with the peak maxima at 241 °C, which can likely be attributed to the sample decomposing. The lack of any additional peaks, aside from those corresponding to the sample melting and subsequently decomposing, indicates that Ni(dbda)₂ does not appear to exhibit liquid-crystalline behaviour.

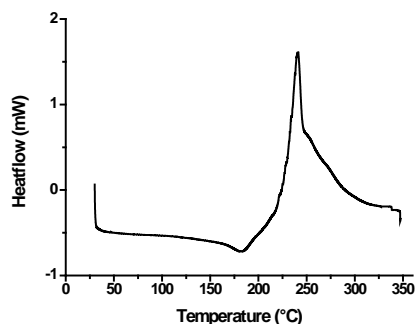


Figure 8 DSC of Ni(dbda)₂ between 25-350 °C.

Calculations have been carried out on Ni(dbda)₂ to estimate the energies of the HOMO and LUMO orbitals and to assign the transitions witnessed in the electronic absorption spectra. To save computational time, these calculations were carried out on molecules carrying ethoxy substituents instead of dodecyloxy substituents; this slight modification should not impact significantly on the predicted electronic structure, from gas phase calculations. From Figure 9 it can be seen that Ni(dbda)₂ has a fairly delocalised electronic structure. In the case of the LUMO (Figure 9 (top)) the wave functions are delocalised over the entire molecule with both metal and ligand contributions. In contrast, the HOMO is also delocalised but mainly ligand based. The energy of the HOMO has been calculated as -3.99 eV and the LUMO as -2.44 eV, with respect to the vacuum level. The calculated HOMO-LUMO gap is somewhat greater than the gap of approximately 1 eV measured electrochemically, attributed to the calculations being carried out in vacuum. The energy of the HOMO orbital indicates that the complex is likely to be easily oxidisable, perhaps explaining its instability under atmospheric conditions.

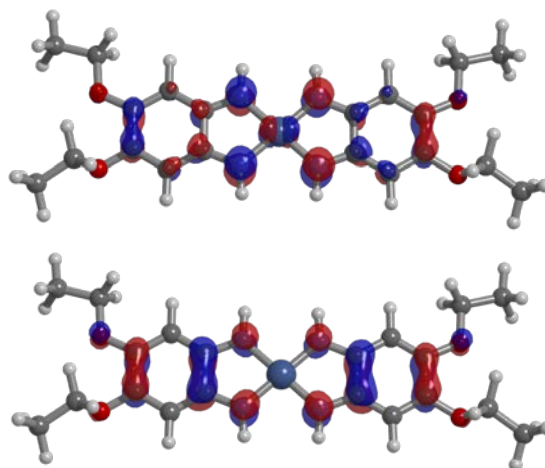


Figure 9 The LUMO (top) and HOMO (bottom) of Ni(dbda)₂

TD-DFT calculations on Ni(dbda)₂ were carried out using the functional B3LYP/6-31G(d,p) in vacuum. The calculation gives an approximate reproduction of the experimental spectrum, albeit with the HOMO-LUMO transition observed at 671 nm rather than the NIR region of the spectrum (Figure 10). Re-calculating the absorption spectrum using a polarisable continuum model (PCM) for DCM provides a closer match to the experimental data in terms of the lambda max peak position at 921 nm. Experimentally, this transition was recorded in DCM at 1024 nm with a molar extinction coefficient around 8500 L mol⁻¹ cm⁻¹.

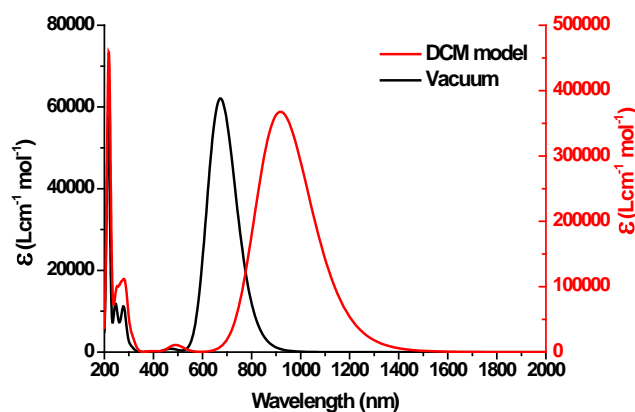


Figure 10 TD-DFT calculation carried out at the B3LYP/6-31G(d,p) level of theory.

To assess charge-transport capability, the Ni(dbda)₂ complex was deposited onto FET substrates via both spin coating and drop casting from solutions of 12 mg/L of analyte in 1,2-dichlorobenzene and 12 mg/L of analyte in 1,2-dichloroethane. Two different FET configurations were used; one with Au source and drain electrodes with a width and gap of 4 μm and the other with a width and gap of 8 μm. However, regardless of FET type employed or solvent system use for film fabrication, insulating device behaviour was observed in every instance with no gate effect. The lack of conductivity in a device may be attributed to several factors: possibly a consequence of the large mismatch in energy between the electrodes (~5.1 eV vs. vacuum)¹⁶ and the frontier orbitals of the complex; the molecular orientation on the substrate may be unsuitable or the material may be intrinsically insulating. The large alkyl chains may also fold over the molecule and impede intermolecular interactions necessary for charge transport.

3. CONCLUSIONS

The syntheses of near-IR absorbing metal-*bis*-1,2-diimine complexes, M(dbda)₂, has been reported. This class of novel complexes represent a significant modification to the already known family of metal bis-ligand diimine complexes, with the addition of electron-donating alkoxy groups leading to near-IR absorption properties, and also facile film formation by drop or spin coating. Electrochemical and optical analysis revealed that Ni(dbda)₂ possesses a small HOMO-LUMO gap, with an oxidative process at low potential measured electrochemically. FET studies indicated that the Ni(dbda)₂ complex was electrically insulating in an FET device with Au electrodes. Likewise, the thin film absorption spectroscopy studies showed no red shifting of the HOMO-LUMO transition indicating that intermolecular interactions were weak. This enables film formation while retaining the optical properties of the parent molecules. Overall, this study opens up the possibility to further study and tune this new complex family in an analogous way to the intensively explored metal-*bis*-1,2-dithiolene analogues.

4. EXPERIMENTAL

4,5-Bis(dodecyloxy)benzene-1,2-diamine (dbdaH₂)

4,5-bis(dodecyloxy)benzene-1,2-diamine was synthesised in three steps, starting from catechol (1,2-dihydroxybenzene), by a previously reported procedure.¹⁷ Catechol (1.99 g, 18 mmol), potassium carbonate (10 g, 72.4 mmol) and 18-crown-6 (0.3 g, 1.1 mmol) were stirred in acetone (100 ml) as 1-bromodecane (9.56 ml, 39.8 mmol) was added dropwise. The resulting white reaction mixture was then heated to reflux for 24 hours under an atmosphere of nitrogen. The solution was filtered hot and the filtrates concentrated under vacuo to leave an off-white solid. The product was then washed with methanol and dried under vacuo. (7.38g, 97% yield). To a cooled, stirring solution of HNO₃ (16 ml, 70%) was added a DCM solution (40 ml) containing the 1,2-bisdodecyloxybenzene product (3.32g, 7.4 mmol) dropwise over a period of 45 minutes. Concentrated H₂SO₄ (8 ml, 95%) was then added dropwise to the dark yellow reaction mixture. After which the reaction mixture was removed from the ice bath and stirred at RT for 2 hours. The orange/brown solution was then poured over ice (200 ml), causing a yellow solid to precipitate out of solution, which was then extracted in DCM (3x150 ml). The organic layer was then washed with saturated NaHCO₃ solution (40 ml) and H₂O (2x40 ml), before being concentrated under reduced pressure to yield a yellow solid (3.81g, 95 % yield). The final step of the reaction involves reducing the dinitroarene (1.25 g, 2.3 mmol) with Pd/C (10 %, 0.43 g) and hydrazine monohydrate (4.24 g, 4.8 mmol) in EtOH (175 ml). The reaction was carried out at 80 °C for 16 hours under an atmosphere of nitrogen. The hot solution was filtered through celite and the filtrate concentrated under reduced pressure to yield an off-white solid. The solid was washed with MeOH (20 ml) and collected by filtration (1.02 g, 93 % yield). ¹H NMR (CDCl₃): δ (ppm) = 0.88 (t, 3H, 7 Hz), 1.30 (m, 16H, 7.5 Hz), 1.43 (m, 2H, 7 Hz), 1.74 (m, 2H, 7 Hz), 3.88 (t, 2H, 6.5 Hz), 6.38 (s, 1H). MS (ESI): m/z (%) = 476.6 (100%) [M+H]⁺.

Ni(dbda)₂

Ni(NO₃)₂·6H₂O (0.128 g, 0.44 mmol) and 4,5-bis(dodecyloxy)benzene-1,2-diamine (0.418 g, 0.87 mmol) were stirred in MeOH (30 ml) under an air atmosphere. The yellow suspension was heated to reflux as triethylamine (0.5 ml, 3.6 mmols) was added dropwise. Within a few minutes the reaction mixture had turned a dark brown colour. The resulting reaction mixture was refluxed for one hour before being cooled to RT. The product was poured into hexane: water (1: 1, 200 ml) with the organic layer extracted, then washed with MeOH (2 x 100 ml) and H₂O (3 x 100 ml). The hexane was removed under vacuum and the sample purified by size exclusion chromatography on Bio-Beads SX-3 using DCM as eluent. (65 mg, 15 % yield). MS (ESI): m/z (%) = 1005.66 (100.00%) [M+H]⁺. ¹H NMR (CDCl₃): δ (ppm) = 0.91 (t), 1.29 (br s), 1.44 (br s), 1.60 (br s), 1.75 (br s), 3.67 (br s). Calculated for C₆₀H₁₀₈NiN₄O₄, C 71.48, H 10.80, N 5.56; found C 71.38, H 10.68, N 5.62. Melting point: 187-189 °C.

Cu(dbda)₂

Cu(NO₃)₂·3H₂O (0.241 g, 1 mmol) and 4,5-bis(dodecyloxy)benzene-1,2-diamine (0.952 g, 2 mmol) were stirred in MeOH (60 ml) under an air atmosphere. The pale green suspension was heated to reflux as triethylamine (1.11 ml, 8 mmols) was added dropwise. The reaction mixture turned dark blue almost immediately following addition of base. Refluxing was continued for one hour before the reaction mixture was cooled to RT, and poured into hexane: water (1: 1, 300 ml). The organic fraction was extracted and washed with MeOH (100 ml), DMF (100 ml x 2) and water (2 x 100ml). The product was concentrated under vacuum and purified by size exclusion chromatography on Bio-Beads SX-3 using DCM as eluent (111 mg, 11 % yield). MS (ESI): m/z (%) = 1011.70 (100.00%) [M+H]⁺. Melting point: 164-165 °C.

Pd(dbda)₂

Anhydrous Pd(Cl)₂ (0.089 g, 0.5 mmol) and 4,5-bis(dodecyloxy)benzene-1,2-diamine (0.476 g, 1 mmol) were stirred in MeOH (30 ml) under an air atmosphere. The reaction mixture was heated to reflux as triethylamine (0.57 ml, 4.1 mmol) was added dropwise. After several minutes the brown/red suspension turned dark green, almost black. The reaction mixture was refluxed in air for one hour before cooling to RT and pouring into DCM: water (1:1, 200 ml). The organic layer was extracted and washed with water (2 x 100 ml) before being dried under vacuum. The crude solid was redissolved in hexane (50 ml) and further washed with MeOH (2 x 100 ml). The hexane layer was evaporated to dryness and the product purified by size exclusion chromatography on Bio-Beads SX-3 using DCM as eluent. (21 mg, 4 % yield). MS (ESI): m/z (%) = 1053.55 (39.18%) [M+H]⁺. ¹H NMR (CDCl₃): δ (ppm) = 0.90 (t, 3H), 1.29 (s, 20H), 1.59 (t, 2H), 3.67 (s, 1H). Calculated for C₆₀H₁₀₈PdN₄O₄, C 68.25, H 10.31, N 5.31; found C 63.08, H 9.71, N 4.94. Melting point: 169-170 °C.

Experimental methods

All cyclic voltammetry measurements were carried out in dry DCM using 0.3 M TBABF₄ electrolyte in a three electrode system, with each solution being purged with N₂ prior to measurement. The working electrode was a Pt wire surrounded by a plastic casing with an exposed surface area of 2 mm in diameter. The reference electrode was Ag/AgCl calibrated against ferrocene/ferrocenium in the background electrolyte, and the counter electrode was a Pt rod. All measurements were made at room temperature using a μAUTOLAB Type III potentiostat, driven by the electrochemical software GPES. Absorption spectroscopy was recorded using a Jasco V-670 UV/Vis/NIR spectrophotometer. Differential scanning calorimetry (DSC) was carried out between 25-300 °C by Dr John Liggat using a DSC Q1000. Measurements were carried out in aluminium pans using nitrogen as the carrier gas. Single point and geometry optimisation calculations of the isolated complexes were carried out at the B3LYP/6-31G(d,p) level of theory,^{18,19,20} using Gaussian 09.²¹ Time-dependent DFT calculations were carried out using the polarisable continuum model (PCM) for DCM which takes into account the effect of solvation. The molecular orbital isosurfaces were visualised using ArgusLab 4.0.²² Thin films for FET measurements were prepared by spin coating using a WS-650S-6NPP/LITE spin coater made by Laurell Technologies. Films were prepared by rotating at 500 RPM for 30 seconds, followed by 2000 RPM for a final 30 seconds. Glass slides were cleaned by sonication for 15 minutes in solutions of decongestant, deionised water, IPA, acetone and CHCl₃. OTS treatment was accomplished by placing dry glass slides into a 5 mmol solution of OTS in anhydrous toluene for 16 hours under an atmosphere of N₂, before removing the slides and carefully rinsing with acetone and CHCl₃. For FET characterisation, a bottom contact (Au), bottom gate configuration was used. A heavily doped silicon wafer served as both the substrate and gate electrode, with a 300 nm thermally grown SiO₂ layer as the gate dielectric. FET substrates were cleaned by soaking in solutions of IPA, acetone and CHCl₃ for 5 minutes each before being dried under a stream of N₂. Two FET configurations were used, both used interdigitated source and drain electrodes; one possessed an electrode width and gap of 4 μm and the other with an electrode width and gap of 8 μm.

5. REFERENCES

- [1] U. T. Mueller-Westerhoff, B. Vance, Y. Dong, *Tetrahedron*, **1991**, *47*, 909
- [2] J-F. Bai et al, *J. Mater. Chem.*, **1999**, *9*, 2419; Z. R. Sun et al, *Chem. Phys. Lett.*, **2001**, *342*, 323; A. Rogalski, K. Chrzanowski, *Opto-Electronics Review* **2002**, *10*, 111
- [3] C. G. Granqvist, I. B. Pehlivan, Y-X. Ji, S. Y. Li, G. A. Niklasson, *Thin Solid Films*, **2014**, *559*, 2
- [4] B-B. Cui, C-J. Yao, J. Yao, Y-W Zhong, *Chem. Sci.*, **2014**, *5*, 932
- [5] D. Espa, L. Pilia, L. Marchiò, M. Pizzotti, N. Robertson, F. Tessore, M. L. Mercuri, A. Serpe, P. Deplano, *Dalton. Trans.*, **2012**, *41*, 12106

- [6] E. Allwright, G. Silber, J. Crain, M. M. Matsushita, K. Awaga, N. Robertson, *Dalton Trans.*, **2016**, 45, 9363
- [7] S. Dalgleish, J. G. Labram, Z. Li, J. Wang, C. R. McNeil, T. D. Anthopoulos, N. Greenham, N. Robertson, *J. Mater. Chem.*, **2011**, 21, 15422
- [8] U. T. Mueller-Westerhoff, B. Vance *Comprehensive Coordination Chemistry*, Pergamon, Oxford, UK 1987
- [9] S. Dalgleish, N. Robertson, *Chem. Commun.*, **2009**, 5826
- [10] Y. Konno, N. Matsushita, *Bull. Chem. Soc. Japan* **2006**, 79, 1046
- [11] L. F. Warren, *Inorg. Chem.* **1977**, 16, 2814
- [12] O. Carugo, K. Djinovic, M. Rizzi, C. B. Castellani, *J. Chem. Soc. Dalton Trans.*, **1991**, 1551
- [13] S.-I. Noro, H.-C. Chang, T. Takenobu, Y. Murayama, T. Kanbara, T. Aoyama, T. Sassa, T. Wada, D. Tanaka, S. Kitagawa, Y. Iwasa, T. Akutagawa, T. Nakamura, *J. Am. Chem. Soc.*, **2005**, 127, 10012
- [14] S.-I. Noro, T. Takenobu, Y. Iwasa, H.-C. Chang, S. Kitagawa, T. Akutagawa, T. Nakamura, *Adv. Mater.*, **2008**, 20, 3399
- [15] F. Lej, G. Morelli, G. Ricciardi, M. F. Brigatti, A. Rosa, *Polyhedron*, **1989**, 8, 2603
- [16] S.-H. Lee, W.-C. Lin, C.-J. Chang, C.-C. Huang, C.-P. Liu, C.-H. Kuo, H.-Y. Chang, Y.-W. You, W.-L. Kao, G.-J. Yen, D.-Y. Kuo, Y.-T. Kuo, M.-H. Tsai, J.-J. Shyue, *Phys. Chem. Chem. Phys.*, **2011**, 13, 4335
- [17] A. Wicklein, M.-A. Muth, M. Thelakkat, *J. Mater. Chem.*, **2010**, 20, 8646
- [18] A. D. Becke, *J. Chem. Phys.*, **1993**, 98, 5648
- [19] C. Lee, W. Yang, R. G. Parr, *Phys. Rev. B*, **1988**, 37, 785
- [20] Ditchfield, R.; Hehre, W. J.; Pople, J. A., *The Journal of Chemical Physics* 1971, 54, 724-728.
- [21] M. J. Frisch, *et al*, Gaussian 09, Revision B.01. In Gaussian 09, Revision B.01, Gaussian, Inc., Wallingford CT, Wallingford CT, 2009.
- [22] M. A. Thompson, ArgusLab 4.0.1, Planaria Software LLC: Seattle, WA.